ARCHIVES of FOUNDRY ENGINEERING

Published quarterly as the organ of the Foundry Commission of the Polish Academy of Sciences

ISSN (1897-3310)
Volume 13
Special Issue
1/2013
73–82

14/1

Structures of the EL-Hard Padding Welds as a Function of the Abrasive Wear Resistance

J. Napiórkowski [a], Ł. Konat [b,] *, G. Pękalski [b], K. Kołakowski [a]

[a] Department of Building, Operation of Vehicles and Machinery, University of Warmia and Mazury in Olsztyn, M. Oczapowskiego 11, 10-736 Olsztyn, Poland
[b] Institute of Materials Science and Applied Mechanics, Wroclaw University of Technology, M. Smoluchowskiego 25, 50-370 Wrocław, Poland
* Corresponding author. E-mail address: lukasz.konat@pwr.wroc.pl

Received 23.04.2013; accepted in revised form 08.05.2013

Abstract

In this work we report the phase structures of the EL-Hard padding weld layers and their effect on their abrasive wear resistance. The application of light and electron scanning microscopy examinations revealed subtle differences in the structures of the padding welds which affect their strength and usable properties. Abrasive wear resistance tests utilizing a "spinning bowl" method performed in real soil masses and hardness tests showed a close relationship between the abrasive wear resistance values and chemical composition of the tested padding welds. The obtained results are explained by the presence of the carbide - forming elements such as B, Cr, Mo, Nb, V and W in the chemical composition and types of the carbide phases present in the structures of the EL-Hard padding welds.

Keywords: Wear resistant alloys, Padding weld layers, Operational characteristics, Mechanical properties, Structural properties

1. Introduction

Issues of the abrasive wear resistance of the padding weld layers in relation to macro- and microstructure have already been followed for several years within the framework of cooperation between Institute of Materials Science and Applied Mechanics of Wrocław University of Technology and Department of Building, Operation of Vehicles and Machinery of the University of Warmia and Mazury in Olsztyn. Cooperation concerns mainly forecasting and operation behavior assessment of the padding weld layers working in lignite mine and soil abrasive mass conditions. There are following stages of the padding weld layers suitability studies for specific use in abrasive wear conditions:

- Analysis of possible structures of the padding weld layers on the ground of electrode chemical composition based on the appropriate phase equilibrium diagrams.
- Metallographic examinations of the padding weld layers specifying their phases and structures allowing for establishment of tendency to form macro- and microscopic (micro-cracks, defects of weld penetration) non-compliances.
- Hardness measurements of abrasive wear on cross-section of the padding weld layers allowing for forecasting of their wear.
- Laboratory wear tests performed in a specific environment verified, if such possibility exists, by adequate operation tests.

Starting point for research is the analysis of phase equilibrium diagrams and examinations of phases and structures of the

padding weld layers [1]. It prevents making random solutions or decisions based exclusively on catalog data - imprecise information of advertising nature.

In the past several years as a result of research on low-alloy martensitic steels (mainly Hardox steels) a problem appeared regarding competitiveness and relations between weld overlay layers and these modern materials in abrasive wear conditions. The problem is particularly interesting once dynamic loadings [2, 3] are present during the course of the wear process. A subject of research reported in this work is on the weld overlay layers executed with coated electrodes for pad welding and rebuilding EL-Hard recognized in PN-EN 14700 and DIN 8555 standards.

Chemical composition of the EL-Hard padding welds is based on Fe-Cr-C alloys. They also contain, depending on the grade, such additives as: Nb, B, W, V, Mo, Si. Padding welds were applied to a pad made of 38GSA grade of steel. Table 1 shows chemical composition of the electrodes and their hardness as specified by the manufacturer.

Table 1.
Chemical composition and hardness of the electrodes used for making the padding welds

Elem. [%]	EL-Hard 61	EL-Hard 63	EL-Hard 65	EL-Hard 67	EL-Hard 70
C	5.2	4.5	4.5	5.0	5.0
Si	2.2	–	1.2	1.5	–
Cr	29.0	34.0	24.0	23.0	38.0
V	–	–	1.0	10.0	–
Nb	6.8	–	6.2	–	–
Mo	–	–	6.0	–	–
W	–	–	2.0	–	–
B	–	–	–	–	3.5
Other	3.5	–	–	–	–
Fe	Rest	Rest	Rest	Rest	Rest
HRC	63-65	61-63	63-65 45*	NA	66-67 60**
* at +400°C, ** at +600°C					

As can be seen in Table 1 the carbon and chromium contents in tested padding welds are in the 4.5-5.2% and 23-38% range, respectively. Both, chromium and other alloying additives have an effect on stabilization of the alloy ferrite in these materials, forming at the same time carbide phases of complex (primary and secondary - e.g. Cr) and simple (e.g. V, Nb) structures. Therefore, the phase structure of the tested padding welds solidifying close to equilibrium conditions should be composed of alloy ferrite and various (alloy) carbides.

The padding welds should exhibit in the main part of their thickness hypereutectic structures, e.g. ledeburite with precipitated primary chromium carbides. In the case of presence of carbide-forming alloying additives other than chromium (in the amount higher than their solubility limit in ferrite) the structure of padding welds will also contain other carbide phases.

2. Macroscopic evaluation results

Macroscopic observations of the padding weld layers were conducted with the Neophot 32 optical microscope (OM) and the SMT 800 stereoscopic microscope working with Nikon Coolpix 990 digital camera and Visitron Systems digital video camera. Macroscopic examinations were performed on the cross sections of all the tested samples of the weld overlay layers. Fig. 1-5 show their macrostructure in regions exhibiting inconsistencies, which might have an effect on their operating durability.

Among five types of padding welds only two did not show the presence of micro-cracks or lack of depth of fusion. They are: EL-Hard 63 (Fig. 2) and EL-Hard 67 (Fig. 4). Maximum intensity of macroscopic defects has been found in the padding weld EL-Hard 65 (Fig. 3) in which beside the micro-cracks propagating through the entire thickness of the padding weld there were also present the defects of depth of fusion.

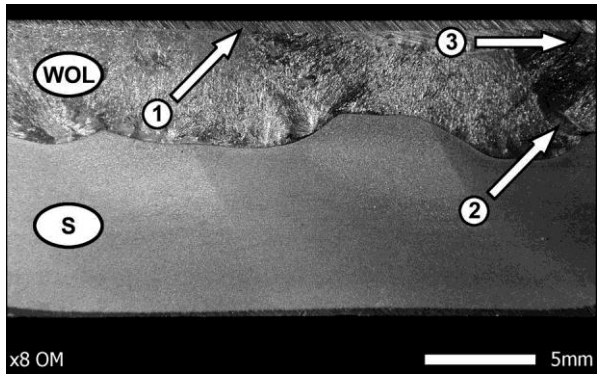

Fig. 1. Macroscopic image of the EL-Hard 61 weld overlay layer. Grinding marks (1), macro-cracks (2) and (3) are revealed. WOL - weld overlay layer, S - substrate. Etched with Mi1Fe and electrolytically with chromic acid, OM

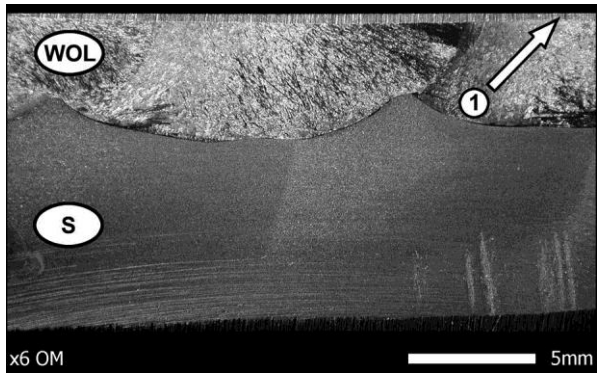

Fig. 2. Macroscopic image of the EL-Hard 63 weld overlay layer. Grinding marks (1). Macroscopic cracks were not found. WOL - weld overlay layer, S - substrate. Etched with Mi1Fe and electrolytically with chromic acid, OM

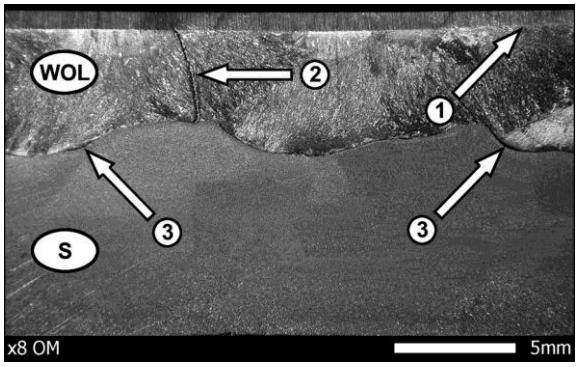

Fig. 3. Macroscopic image of the EL-Hard 65 weld overlay layer. Grinding marks (1). In the padding weld are visible extensive macro-cracks (2) reaching the material of the substrate. Along the fusion line are visible discontinuities of weld penetration (3). WOL - weld overlay layer, S - substrate. Etched with Mi1Fe and electrolytically with chromic acid, OM

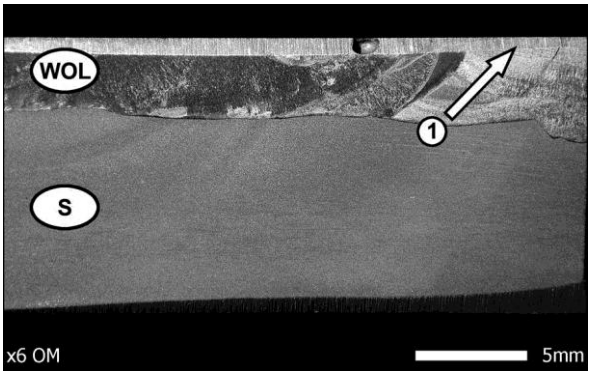

Fig. 4. Macroscopic image of the EL-Hard 67 weld overlay layer. Grinding marks (1). Macroscopic cracks were not found. WOL - weld overlay layer, S - substrate. Etched with Mi1Fe and electrolytically with chromic acid, OM

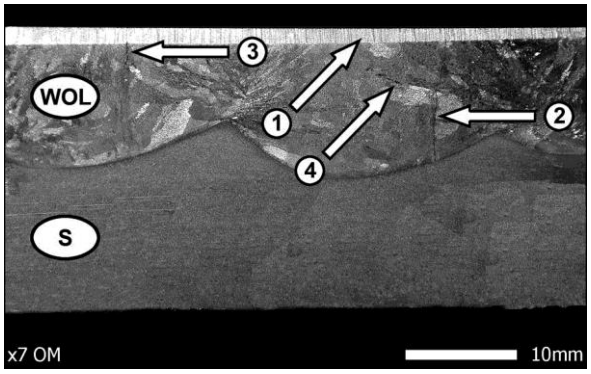

Fig. 5. Macroscopic image of the EL-Hard 70 weld overlay layer. Grinding marks (1). In the padding weld are visible two extensive macro-cracks (2) and (3) and numerous small and scattered discontinuities (4). WOL - weld overlay layer, S - substrate. Etched with Mi1Fe and electrolytically with chromic acid, OM

3. Microscopic evaluation results

For observations of the microstructures the Neophot 32 optical microscope (OM) was used in the magnification range of 25-2 000 times. Images of the microstructures were registered with the Visitron Systems digital camera with the use of Spot Advanced software. Microstructure observations at higher magnifications and analysis of chemical composition, morphology and phase identification were conducted with the JEOL JSM-5800LV scanning electron microscope (SEM) coupled with the Oxford LINK ISIS-300 X-ray microprobe analyzer. The accelerating voltages were 20 and 25kV. Microstructural observations were conducted with material contrast using SE and BSE detectors. The samples were sputtered with amorphous carbon for SEM observations.

3.1. EL-Hard 61 weld overlay layers

Microscopic structure of the padding weld executed with the EL-Hard 61 electrode is presented on the micrographs shown below.

Fig. 6 shows the end portion of the micro-crack marked as (3) in Fig. 1. Except for a narrow "strip" of the alloy ferrite from which fine dendrites of this phase grow into the padding weld material, the padding weld is characterized by homogenous structure (Fig. 6 and 7). Together with ledeburite there are also large primary precipitates of chromium and niobium carbides (Fig. 8).

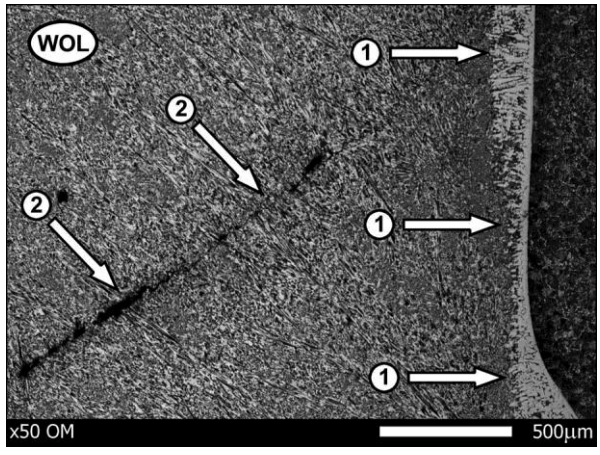

Fig. 6. Microscopic image of the fusion zone of the EL-Hard 61 padding weld. Clearly defined "strip" of alloy ferrite (1) in the fusion zone and section of the crack (2) visible in the layer of the weld overlay. WOL - weld overlay layer. Etched with Mi1Fe and electrolytically with chromic acid, OM

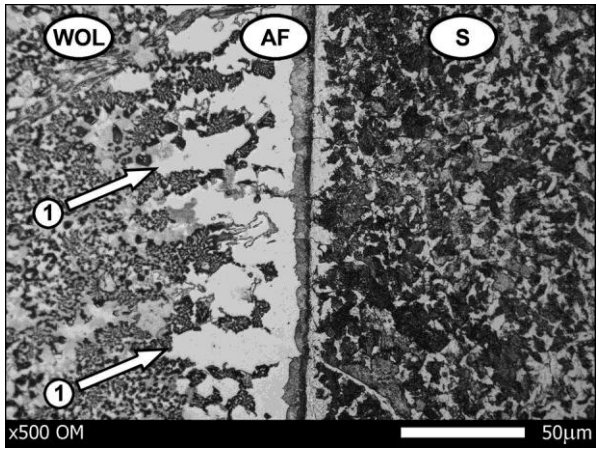

Fig. 7. Microscopic image of the fusion zone of the EL-Hard 61 padding weld. Magnification of the portion of the fusion zone shown in Fig. 6. At the joint of the padding weld and the substrate material there is a "strip" of alloy ferrite from which dendrites of this phase solidified into the padding weld material (1). Microstructure of the substrate material is comprised of bright ferrite grains with dark regions of dense lamellar perlite. WOL - weld overlay layer, AF - alloy ferrite, S - substrate. Etched with Mi1Fe and electrolytically with chromic acid, OM

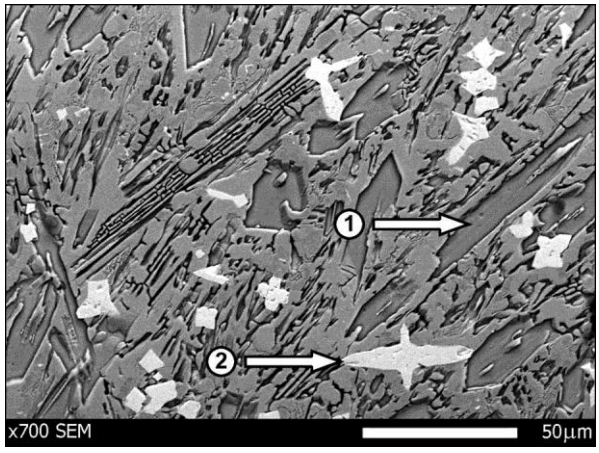

Fig. 8. Microscopic image of the EL-Hard 61 weld overlay layer. Magnification of the portion of the fusion zone shown in Fig. 9. Microstructure of the weld overlay layer showing precipitates of chromium (1) and niobium (2) carbides. Etched with Mi1Fe and electrolytically with chromic acid, SEM

3.2. EL-Hard 63 weld overlay layers

In the fusion zone (Fig. 9) the weld overlay layer has similar structure to the corresponding zone of the padding weld executed with the EL-Hard 61 electrode. However, microcracks (2) have been found in the alloy ferrite "strip" as shown in Fig. 9. Beyond the region shown in Fig. 9, the weld overlay layer is composed of ledeburite and primary chromium carbides (Fig. 10).

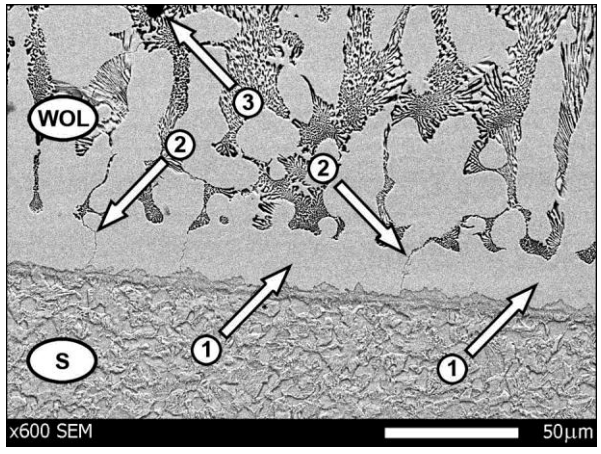

Fig. 9. Microscopic image of the fusion zone of the EL-Hard 63 weld overlay layer. A "strip" of the alloy ferrite (1) in the padding weld with visible micro-cracks (2) and single gas bubble (3). WOL - weld overlay layer, S - substrate. Etched with Mi1Fe and electrolytically with chromic acid, SEM

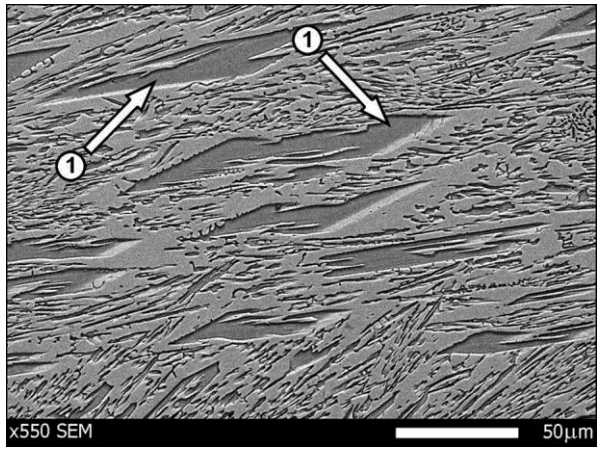

Fig. 10. Microscopic image of the EL-Hard 63 weld overlay layer. Large precipitates of the primary chromium carbides (1) against mixture of the alloy ferrite and carbides. Hypereutectic Fe-Cr-C alloy of ledeburitic structure. Etched with Mi1Fe and electrolytically with chromic acid, SEM

3.3. EL-Hard 65 weld overlay layers

In due course of macroscopic examination the extensive cracks and local lack of depth of fusion have been found in the padding weld executed with the EL-Hard 65 electrode (Fig. 11). At the same time, it is the padding weld executed with the electrode of most complex chemical composition (Table 1) containing strong carbide-forming additives: V, Nb, Mo, W. Therefore, already in the fusion zone (Fig. 12 and 13), besides chromium carbides and alloy ferrite, there are also different types of carbides.

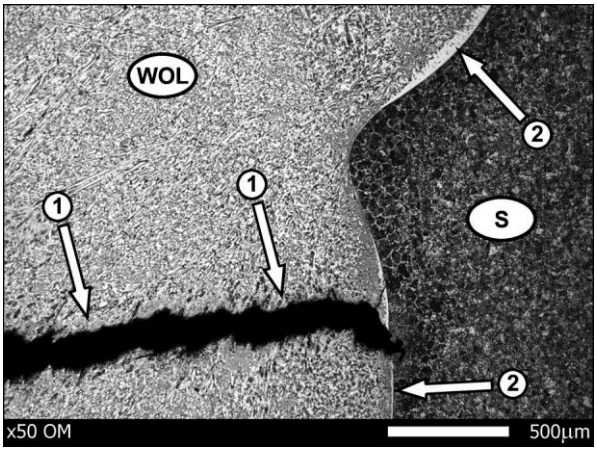

Fig. 11. Microscopic image of the fusion zone of the EL-Hard 65 weld overlay layer. Macro-crack (1) propagating through the thickness of the padding weld and partially penetrating into the substrate material. Locally occurring a "strip" of the alloy ferrite (2). WOL - weld overlay layer, S - substrate.
Etched with Mi1Fe and electrolytically with chromic acid, OM

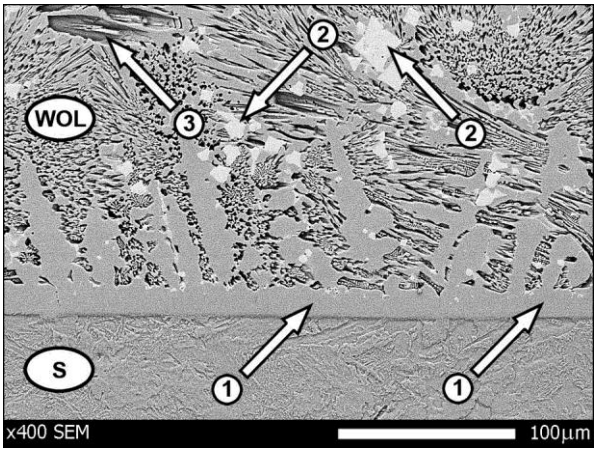

Fig. 12. Microscopic image of the fusion zone of the EL-Hard 65 weld overlay layer. Visible "strip" of the alloy ferrite (1) in the padding weld and several types of carbides (2) and (3).
WOL - weld overlay layer, S - substrate.
Etched with Mi1Fe and electrolytically with chromic acid, SEM

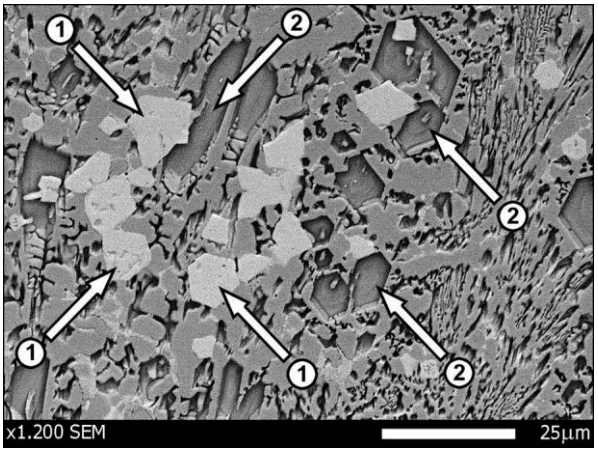

Fig. 13. Microscopic image of the EL-Hard 65 weld overlay layer. Mixture of the alloy ferrite and niobium carbides (1) and carbides of the type M_7C_3 (Fe, Cr_7C_3) (3).
Etched with Mi1Fe and electrolytically with chromic acid, SEM

3.4. EL-Hard 67 weld overlay layers

In due course of microscopic examination the presence of microcracks marked (2) in Fig. 14, unidentifiable macroscopically, has been revealed in the weld overlay layer executed with the EL-Hard 67 electrode. Beyond the region of fusion zone the tested padding weld has microstructure composed of ledeburite, primary chromium carbides and vanadium carbide precipitates (Fig. 15 and 16).

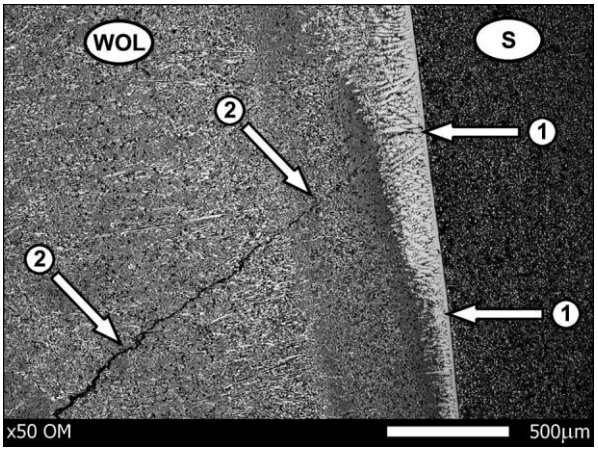

Fig. 14. Microscopic image of the fusion zone of the EL-Hard 67 weld overlay layer. Visible "strip" of the alloy ferrite (1) in the padding weld with dendrites of this phase of variable length. Micro-crack (2) propagating through the entire thickness of the padding weld. WOL - weld overlay layer, S - substrate.
Etched with Mi1Fe and electrolytically with chromic acid, OM

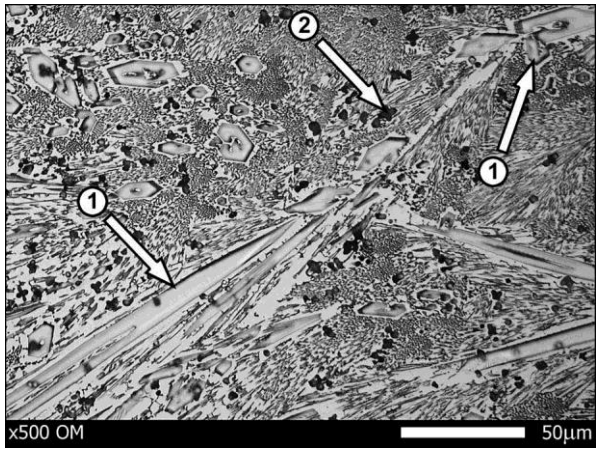

Fig. 15. Microscopic image of the EL-Hard 67 weld overlay layer. The alloy ferrite with carbides (the structure of ledeburitic mixture) with unevenly distributed precipitates of the primary chromium carbides (1) and fine vanadium carbides (2). Etched with Mi1Fe and electrolytically with chromic acid, OM

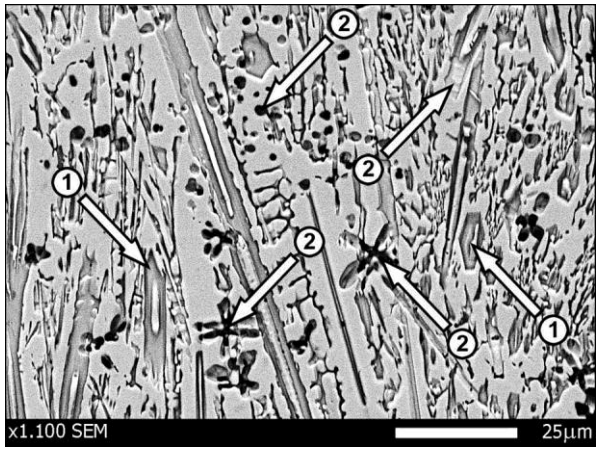

Fig. 16. Microscopic image of the EL-Hard 67 weld overlay layer. Ledeburitic mixture of the alloy ferrite and chromium carbides of the M_7C_3 type (1) and vanadium carbides (2). Etched with Mi1Fe and electrolytically with chromic acid, SEM

3.5. EL-Hard 70 weld overlay layers

Fig. 17 and 18 show characteristic microstructural features of the weld overlay layer executed with the EL-Hard 70 electrode. Extensive macro- and micro-cracks have been found in both the padding weld and the substrate material (Fig. 17). Beyond the fusion zone the padding weld has ledeburitic structure with large precipitates of the primary chromium carbides and few fine boron carbides (Fig. 18).

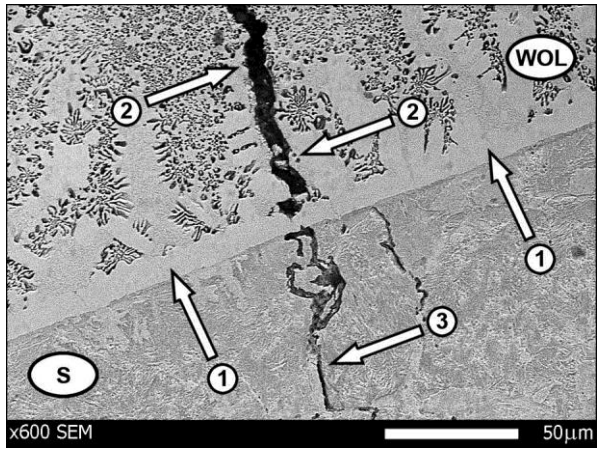

Fig. 17. Microscopic image of the fusion zone of the EL-Hard 70 weld overlay layer. Clearly visible "strip" of alloy ferrite (1) in the fusion zone with single micro-cracks. Extensive micro-crack (2) in the padding weld present also in the substrate material. WOL - weld overlay layer, S - substrate. Etched with Mi1Fe and electrolytically with chromic acid, SEM

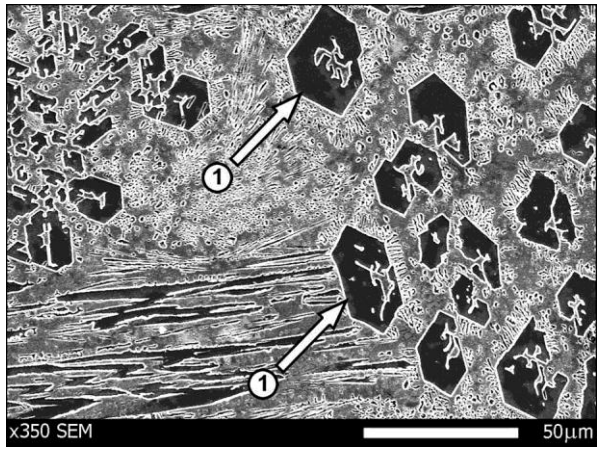

Fig. 18. Microscopic image of the EL-Hard 70 weld overlay layer. Primary precipitates of chromium carbides (1) in the matrix of the mixture of the alloy ferrite and carbides. Etched with Mi1Fe and electrolytically with chromic acid, SEM

4. Hardness variations throughout the thickness of the padding weld

Hardness measurements of the weld overlay layer were made using Vickers method in accordance with PN-EN ISO 6507-1:1999 standard. Measurements were performed using Zwick 32 hardness tester at 1kG (9.807N) load acting for 15s. Position of the hardness measurements (along the A-B line) is schematically shown in Fig. 19.

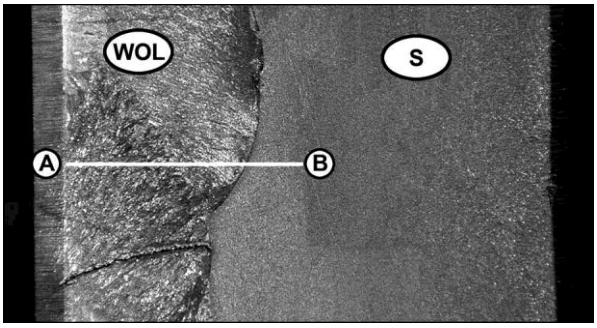

Fig. 19. Schematics of the hardness measurements of the weld overlay layer executed with the EL-Hard electrodes. Hardness distributions were accomplished along the A-B line. WOL - weld overlay layer, S - substrate

Table 2.
Results of the hardness measurements of the weld overlay layers executed with the EL-Hard electrodes

mm	EL-Hard 61	EL-Hard 63	EL-Hard 65	EL-Hard 67	EL-Hard 70
	Hardness [HV/HRC]				
0.5	674/59	720/61	520/50	638/57	697/60
1,0	707/61	617/56	652/58	636/57	622/56
1,5	838/65	633/57	688/60	615/56	664/59
2,0	838/65	560/53	691/60	612/56	519/50
2,5	756/63	592/55	684/60	638/57	578/54
3,0	770/63	254/23	771/63	625/57	573/54
3,5	871/66	239/20	776/63	607/56	595/55
4,0	779/63	241/21	693/60	303/30	520/50
4,5	784/64		652/58	250/22	521/50
5,0	727/61		647/58		580/54
5,5	260/24		637/57		236/20
6,0	241/21		248/22		237/20
6,5			242/21		

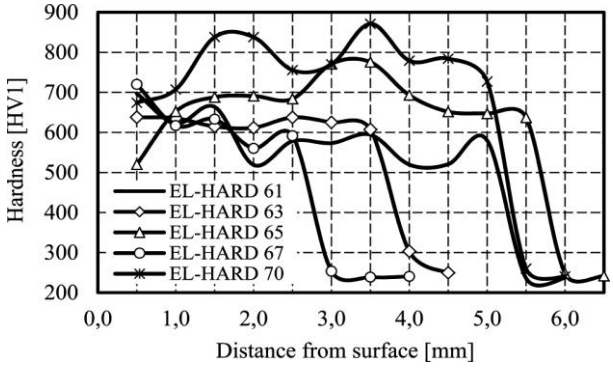

Fig. 20. The course of hardness distributions of the weld overlay layers executed with the EL-Hard electrodes

Hardness measurements show that the tested padding welds exhibit slightly lower values of hardness than those presented by the manufacturer in the data sheets (Table 1). From the course of variation in hardness of the tested padding welds (Table 2 and Fig. 20) becomes obvious that the highest level of hardness shows the EL-Hard 70 (Fe-Cr-B) padding weld and the lowest EL-Hard 61. However, hardness measurements show that hardness variations throughout the padding weld thickness are within the range of 16HRC. Therefore, hardness variations throughout the thickness compare favorably with the results presented in reference [4] since the level of the padding weld hardness is stable. This allows to forecast a steady (linear) course of their wear in progress of the laboratory tests on abrasive wear resistance.

5. Results and analysis of the abrasive wear tests

5.1. Testing methodology

Abrasive resistance wear tests of padding welds were performed in Department of Building, Operation of Vehicles and Machinery of the Warmia and Mazury in Olsztyn University with utilization of the "spinning bowl" method using the MZWM–1 device. Parallelepiped padding weld specimens with dimensions of 30x25x10mm were used for testing, 12 specimens for each type of tested material. Two samples - one of each type of the material - were tested simultaneously in the machine. Total friction distance traveled by each tested sample was 20 000m and the speed approximately 1.7m/s. Specimen mass measurements were performed every 2 000m using a laboratory scale with measuring accuracy of 0.0001g after cleaning in an ultrasonic washer. Each time at this stage of testing the soil mass was exchanged with fresh soil and initial parameters of specimen mass were established. Samples were moving with an oscillatory motion along the friction path. Characteristics of the abrasive soil mass are shown in Table 3. Evaluation of the granulometric composition was executed with Mastersizer 2000+Hydro particle size laser meter and moisture of the soil was determined by measurement of the solid state phase dried at a temperature of 105°C. Tests were conducted using wet abrasive mass.

Table 3.
Characteristics of the abrasive soil mass

Type of soil	Granulometric class	Fraction content [%]			Moisture weight
		Sand 2,0-0,05	Dust 0,05-0,002	Clay <0,002	
		[mm]			[%]
Light	Clay sand	77.48	20.83	1.69	10-12
Medium	Light clay	56.48	30.83	12.69	11-13
Heavy	Plain clay	26.86	48.62	24.52	12-15

5.2. Course of testing

Results of the abrasive wear resistance are shown in Table 4 and Fig. 21-23.

Table 4.
Comparison of the sample mass decrement for the padding welds made with the EL-Hard electrodes on the friction path of 20000m in different abrasive soil masses

Type of padding weld	Type of soil			
	Light	Medium	Heavy	Average
	Sample mass decrement: average – AV [g]; unitary – UN [g/km/cm2]			
EL-Hard 61	0,4824 (0,0032)	0,1634 (0,0011)	0,1913 (0,0013)	0,2790 (0,0019)
EL-Hard 63	0,2741 (0,0018)	0,1549 (0,0010)	0,1136 (0,0008)	0,1809 (0,0012)
EL-Hard 65	0,4650 (0,0031)	0,1607 (0,0011)	0,1465 (0,0020)	0,2574 (0,0020)
EL-Hard 67	0,3669 (0,0024)	0,1472 (0,0010)	0,1355 (0,0090)	0,2165 (0,0042)
EL-Hard 70	0,1568 (0,0010)	0,1910 (0,0013)	0,2289 (0,0015)	0,1922 (0,0013)

Taking into account the average mass decrement values (Table 4) it can be shown that the highest resistance to abrasive wear, independent of the soil type exhibit the padding welds executed with the EL-Hard 63 and EL-Hard 70 electrodes while the largest average mass decrements show the padding welds executed with the EL-Hard 65 and EL-Hard 61 electrodes. Analysis of the abrasive wear resistance tests depending on the type of soil shows that the largest diversity of the average results of mass decrements is present in the light soil (Table 4). In these conditions the best results were obtained for the padding weld made with the EL-Hard 70 and the worst with the EL-Hard 61 electrode. In condition of abrasion in the medium and heavy type of soil the highest average mass decrements show the padding welds made with the EL-Hard 70 electrode while the lowest values of this measure of wear in the medium type of soil exhibits the padding weld made with the EL-Hard 67 electrode and in the heavy soil EL-Hard 63.

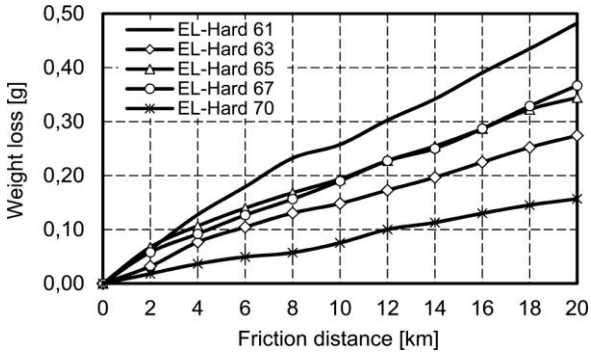

Fig. 21. Mass decrement of the weld overlay layer samples executed with the EL-Hard electrodes. Tests conducted in the light soil mass

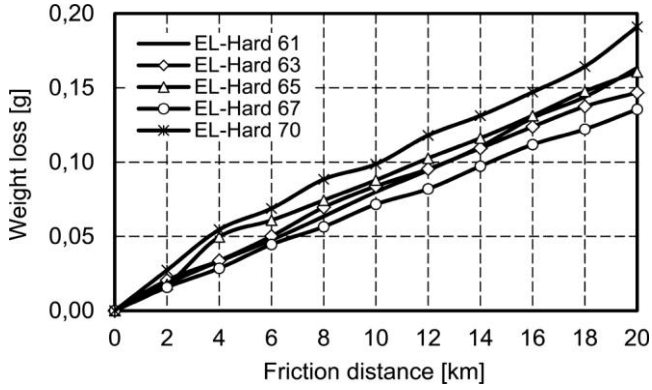

Fig. 22. Mass decrement of the weld overlay layer samples executed with the EL-Hard electrodes. Tests conducted in the medium soil mass

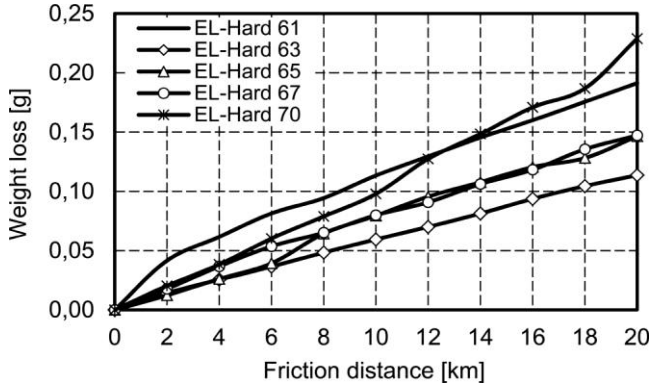

Fig. 23. Mass decrement of the weld overlay layer samples executed with the EL-Hard electrodes. Tests conducted in the heavy soil mass

6. Analysis of the test results and conclusions

Optimal areas of applicability in the exploration conditions of the considered electrodes are determined in the form of appropriate recommendations in the manufacturer data sheets and in the PN-EN 14700 standard. In these recommendations (certainly generally accurate) there are no references to the exploration behavior in abrasive conditions in the soil (e.g. ploughshares). Therefore, testing of the behavior in the soil conditions of the padding welds made with these electrodes seems to be reasonable. In the opinion of the potential users the chemical compositions of the padding welds (electrodes), their microstructure or hardness are irrelevant. Important are the results of the laboratory abrasive wear tests conducted in conditions resembling those of exploration and finally the results of the operational tests themselves. Considering the simple average sample mass decrement in the soil (without taking into account its type) the laboratory test results show the advantage of the padding welds executed with the EL-Hard 63 and the EL-Hard 70

electrodes. The former is the Fe-Cr-C alloy and the latter, besides these elements, also contains the addition of 3.5% boron. In turn, worse abrasive wear resistance results are exhibited by the padding welds made with the electrodes of more complex chemical compositions (EL-Hard 61 and EL-Hard 65). The former is the Fe-Si-Cr-Nb alloy with some other additives and the latter is the Fe-Si-C-V-Nb-Mo-W alloy. In the final considerations we ignore the presence of macroscopic defects in the EL-Hard 63 and EL-Hard 70 padding welds. In the former (Fig. 2) there were no defects of this type found and in the latter they existed (Fig. 5). In the padding weld made with the EL-Hard 70 electrode these defects can be avoided by slight modifications in the pad welding technology (e.g. decrease of cooling rate because of the presence of boron). By adopting these assumptions it can be shown that the best results were obtained for the padding welds of the least complex chemical compositions. Their microstructures (Fig. 10 and 18) consist of the primary precipitates of chromium carbides embedded in the fine-dispersion mixture of the alloy ferrite and the fine carbides (ledeburite) and in case of the EL-Hard 70 electrode also the phases containing boron. Justifying the "worse" behavior of the padding welds made with different electrodes the role of the interphase boundaries in the course of the abrasive wear laboratory tests might be indicated. In each considered case the ferrite strengthening by alloy additives (chromium dissolves in ferrite up to 3.5%) is a positive development. At the same time formation of the subsequent phases under the influence of alloying elements expands the interfacial surface in the padding weld volume. This surface depends not only on the quantity of these phases but also on their shape and morphology (Fig. 16 and 18). It appears likely that in such complex microstructures the process of wear is limited not only by the abrasive wear but also by a discrete (step) removal of carbide phases as a result of their decohesion in the interphase boundaries. If there was no information on the hardness of the padding weld made with the EL-Hard 65 electrode (Table 1) showing its hardness to be 45HRC at 400°C it could be assumed that its chemical composition was designed according to "the more carbides the better" rule.

7. Summary

Results obtained from tests conducted in three different abrasive soil masses show a complexity of the wear process in discrete tribological nodes. Diversification of friction surface is the result of the content of particular soil fractions and their actual state. The highest wear of the weld overlay layers was found in the sand soil. It was approximately 1.4 times higher than the wear in plain clay soil and almost twice higher than in the light clay. It was also found that for the sand soil threefold variations of obtained values of wear for particular padding welds were present. The lowest wear for this abrasion mass showed the padding welds obtained with the EL-Hard 70 and EL-Hard 63 electrodes, which are the welds containing chromium carbides and, in case of the former, also boron compounds. However, the highest values of the wear were found for the weld overlay layers containing strongly carbide-forming and at the same time refractory additives such as V, Nb, Mo, and W. For these sample surfaces besides the presence of chromium carbides and the alloy ferrite other numerous types of carbides were found in the fusion zone.

Causes of the above mentioned relationships need to be sought in the mechanism of the wear. In case of the wear in abrasion mass containing large quantities of silica, there was the largest surface of actual contact with abrasion material. In the wear process phenomenon of the carbide furrow from the alloy ferrite occurred and therefore the increased wear of surface layer. It should be emphasized that the best abrasive wear resistance was obtained for the padding weld with local microcracks (Fig. 14). There was no direct effect of microcracks on the course of the wear for the weld overlay layers. Most of the macro- and micro-cracks were found in the padding welds, which reached the thickness of 5mm. In the padding welds of thickness up to 3.5mm only fine microcracks were observed. Then, it can be stated that together with the increase in the padding weld thickness increases also the risk of occurrence of cracks, which sometimes also extend into the substrate material.

Tested padding welds were characterized by a substantial scatter in hardness on their cross- sections. Most stable properties showed the EL-Hard 63 padding weld. Difference in hardness was only 31HV for the cross-section thickness of 3.5mm whereas for other padding welds it was in the 117-256HV range. For the EL-Hard 70 and EL-Hard 67 padding welds the highest hardness was observed not on the surface but on the cross-section at the distance of above 1mm from the surface and in the latter this increase in hardness was as high as 256HV.

The wear results obtained in the clay soil mass require a different analysis. A friction process in this type of soil had different nature than that in the sand soil. The clay soils show tendency to form soil aggregates hence there are many air pores in the friction space and thus substantially more discontinuities of friction surface than in case of the sand soil. Moreover, the effect of clay and dust itself on the wear process is minimal. However, in the mixture with other fractions this effect undergoes manifold increase. Increased values of the wear in the heavy clay with respect to the values obtained in the light clay resulted from the fact that in this type of the mass bigger soil aggregates formed than in case of the light clay, which resulted in the increase of the friction surface.

Differences in the wear resistance of individual padding welds were not as substantial as in the case of the sand soil and the padding weld made with the EL-Hard 63 electrode confirmed its usability. Differences in the wear of the individual padding weld layers did not exceed 25% and 55% for the light and heavy soil mass, respectively. The highest wear values were found for the padding weld containing chromium and niobium carbides. The essential cause of the intensive wear of this type of the padding weld, especially in the light type of soil, might be the numerous macro-cracks existent in this layer.

The padding weld layers made with the EL-Hard electrodes possess high abrasive wear resistance. The results obtained during laboratory tests should be verified in the real operating conditions since relying upon the obtained data it can be concluded that besides the properties of the padding welds, the type and state of the abrasive soil mass determine the wear process.

References

[1] Pękalska, L. & Pękalski, G. (2000). Phase structure and microstructures of the padding weld used in brown coal mining. *Węgiel Brunatny*. Spec., 86-91.

[2] Alenowicz, J., Dudziński, W. & Pękalski, G. (2000). Structural properties of the padding welds executed with DPT-6 powder electrode and durability of the teeth bucket excavator. *Górnictwo Odkrywkowe*. 42(5/6), 11-18

[3] Napiórkowski, J., Konat, Ł., Pękalski, G. & Kołakowski, K. (2013). Microstructures and wear resistance of the Hardox steels in abrasive soil mass. *Archives of Civil and Mechanical Engineering*. (in press)

[4] Pękalski, G., Napiórkowski, J., Pękalska, L., Kamińska, A. (1997). Padding welds with complex phase structure in relation to abrasive mass wear. *IMMT PWr Report*, SPR(6).